J Mater Sci (2010) 45:5923–5928
DOI 10.1007/s10853-010-4672-4

Combustion synthesis of ferromagnetic Al_2O_3-based cermets in thermal explosion mode

Tao Lu · Ye Pan

Received: 20 January 2010 / Accepted: 28 May 2010 / Published online: 8 June 2010

Abstract The ferromagnetic Al_2O_3-based cermets with different ratios of Co and Co–50Ni alloys were successfully prepared by combustion synthesis in thermal explosion (TE) mode. The reaction process, microstructure, and magnetic property of cermets were investigated. The relative density of cermets can be over 95% via uniaxial loading at the time of ignition when the cermets are hot and ductile. In Al_2O_3–Co cermets, β-Co and α-Co co-exist at room temperature with average size of less than 10 μm and disperse homogeneously in the matrix, while in Al_2O_3–(Co–50Ni) cermets, the network-like Co–50Ni alloy can infiltrate into the boundary gaps of Al_2O_3 particles. The ferromagnetic Co and Co–50Ni alloys are responsible of the magnetic properties of Al_2O_3-based cermets. The saturation magnetization strongly depends on the magnetic characteristics and ratios of ferromagnetic phases. Al_2O_3–(Co–50Ni) cermets have soft magnetic properties with high magnetic susceptibility and low coercive force.

Introduction

Al_2O_3-based cermets reinforced with nano- and submicron-scale metal particles have been studied as structural materials over the past decades [1–3]. Recently, the ferromagnetic Al_2O_3-based cermets, which have homogeneously dispersed ferromagnetic metal or alloy particles in Al_2O_3 matrix, such as Fe, Co, and Ni, are very attractive because on the premise of improving the toughness of monolithic Al_2O_3 ceramic, magnetic properties can be introduce into structural materials [4–6].

Comparing with conventional preparing process for ferromagnetic Al_2O_3-based cermets, such as hot pressing [7] and high-energy ball milling [8], combustion synthesis which takes advantage of the self-sustained high exothermic reaction of reactants is proved to have particular superiority for preparing composites, such as high purity of products, simple processing facilities, low costs of process, and formation of new metastable phases [9]. However, the combustion synthesized products always represent high porosity which is mainly responsible for its inferior mechanical properties and limits the application of products as structural materials. It has been demonstrated that application of pressure during or after the combustion step can considerably increase the product density [10]. Therefore, we use combustion synthesis combined with densification technique to efficiently prepare ferromagnetic Al_2O_3-based cermets and ensure the quality of final product.

In the present work, Al_2O_3–Co and Al_2O_3–(Co–50Ni) cermets were prepared by combustion synthesis in thermal explosion mode. The research focuses on preparing process, microstructures, and magnetic properties of cermets.

Experimental methods

The reactions used to prepare Al_2O_3-based cermets were shown as follows:

$$2Al + Co_2O_3 + 2Al_2O_3 \rightarrow 3Al_2O_3 + 2Co \quad (1)$$

$$10/3Al + Co_2O_3 + 2NiO + 2.8Al_2O_3 \rightarrow 4.47Al_2O_3 + 2Co + 2Ni \quad (2)$$

$$2Al + Co_2O_3 + 2Ni + 1.8Al_2O_3 \rightarrow 2.8Al_2O_3 + 2Co + 2Ni \quad (3)$$

T. Lu · Y. Pan (✉)
Jiangsu Key Laboratory of Advanced Metallic Materials, School of Material Science and Engineering, Southeast University, Nanjing 211189, People's Republic of China
e-mail: panye@seu.edu.cn

27.8 wt.% Co–Al_2O_3 and 34.1 wt.% (Co–50Ni)–Al_2O_3 cermets can be prepared by reaction (1) and reaction (2), respectively, where Al_2O_3 plays the role of diluents. Meanwhile, we directly add pure Ni powder to form Co–50Ni alloy in reaction (3) in purpose of increasing the mass percentage of the metallic phase to about 45.2 wt.%.

Powders of Al, NiO, Co_2O_3, Al_2O_3, and Ni (≥99% purity) used in the experiments with average particle size less than 80 μm as shown in Fig. 1a were originally supplied by SCRC (Sinopharm Chemical Reagent Co. Ltd, PR China). The mixture powders were prepared to get an average particle size of ~1.56 μm by ball milling in alcohol for 8 h as shown in Fig. 1b, then dried and pressed into compacts of Φ20 × 10 mm cylinder with 60% theoretical maximum density (TMD). The green compacts were heated in graphite crucible until the reaction was ignited, and the ignition temperature (T_0) was detected by thermocouple put into the middle of the compact. The cermets were immediately densified by uniaxial loading (~1.28 MPa) at the time of ignition, and the densities of cermets were measured based on Archimedes principle in alcohol. The microstructure and phase composition of cermets were characterized employing X-ray diffraction (XD-3A, SHIMADZU, USA) with Cr K_α radiation (operating at 40 kV and 2°/min) and Sirion Field-emission Scanning Electron Microscope (FEI, Holland) with energy dispersive spectroscopy (EDS). The magnetic hystereses (M–H) of cermets were measured at room temperature using a Quantum Design (USA) vibrating sample magnetometer (VSM) in Physical Property Measurement System (PPMS-9).

Results and discussion

Reaction process

The green compacts are heated from room temperature to ignition temperature (T_0) with the average heating rate of 1.32 °C/s. The temperature evaluation curves as shown in Fig. 2 indicate that T_0 of reaction (1) is about 730 °C,

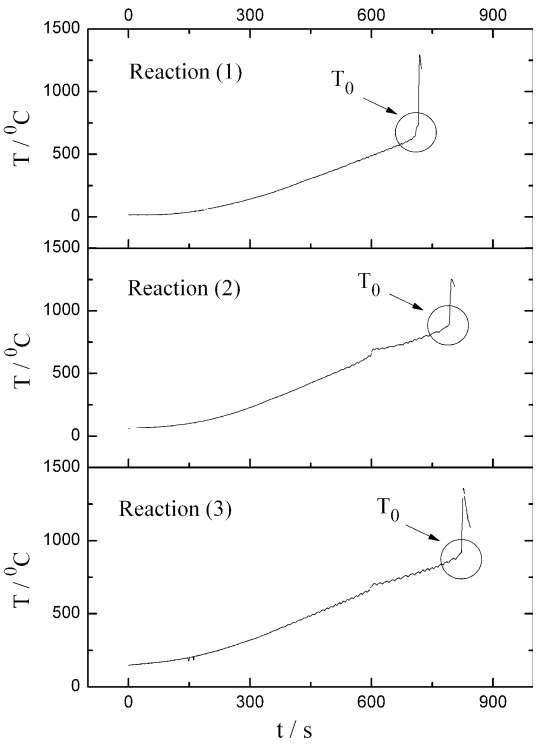

Fig. 2 Temperature evolution curves of all reactions

which is much lower than that of reaction (2) (~892 °C) and reaction (3) (~919 °C). The reasons of such differences are as follows: T_0 of 730 °C in reaction (1) indicates the ignition of Al–Co_2O_3 reaction system; the higher T_0 of 892 °C in reaction (2) is due to the simultaneous ignition of Al–Co_2O_3 and Al–NiO systems that needs more energy supplying; in reaction (3), Ni powder, which is added into the compact in purpose of forming Co–50Ni alloy, plays the role of diluents rather than the reactants, so that T_0 also increases. Subsequently, the rapid vertical raise of the temperature curves of all reactions indicates that the thermal explosion reaction occurs. At this moment, the production of dense cermets can be accomplished by applying uniaxial loading when the products are still hot and ductile. The relative densities of all synthesized cermets are shown in Table 1.

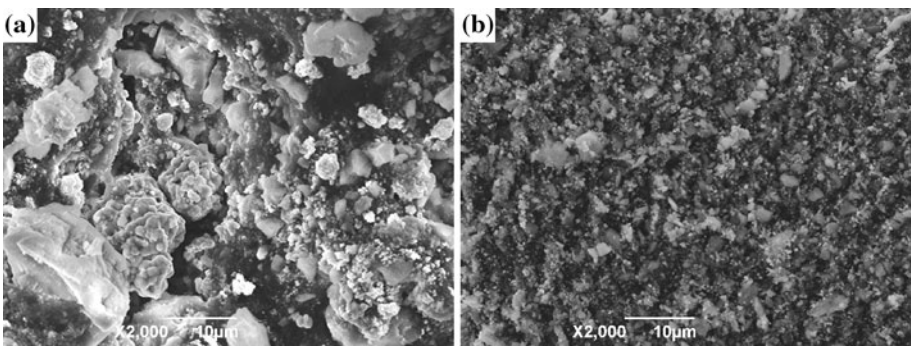

Fig. 1 The morphology of mixture powders (**a** before ball milling, **b** after ball milling)

Table 1 Density data of products

Reaction	Theoretical density/g/cm^3	Measured density/g/cm^3	Relative density/%
(1)	4.52	4.32	95.5
(2)	4.39	4.23	96.3
(3)	5.06	4.81	95

Phases and microstructures

Al_2O_3–Co cermets

The XRD pattern for the cermets synthesized by reaction (1) as shown in Fig. 3 shows that Al_2O_3 matrix and Co metal are obtained by thermite reaction, and the peaks of unreacted Al or Co–Al alloys are not found, that is, Al_2O_3–Co cermets are successfully prepared. Meanwhile, two kinds of allotropic Co phases are both found in the cermets. Prior work has found that the strain (or stress) plays the significant role in the allotropic transformation from β-Co to α-Co [11]. Therefore, high-temperature stable β-Co is firstly synthesized in combustion reaction [12] and then during the cooling stage, a part of β-Co particles are preserved by rapid heat loss through graphite crucible and the others are transformed to α-Co due to the inner heat stress of cermets. The XRD result also shows that the unexpected $CoAl_2O_4$ spinel phases exist in the cermets.

Figure 4 shows the microstructure and EDS data of Al_2O_3–Co cermets. The intending Co particles with average size of less than 10 μm disperse homogeneously in the Al_2O_3 matrix with solid solution of spinel phases. The approximate sphere Co particles are formed by the in-situ synthesized liquid Co agglomerating from adjacent region under high reaction temperature. However, the bulk agglomerated Co particles are not found because of Al_2O_3

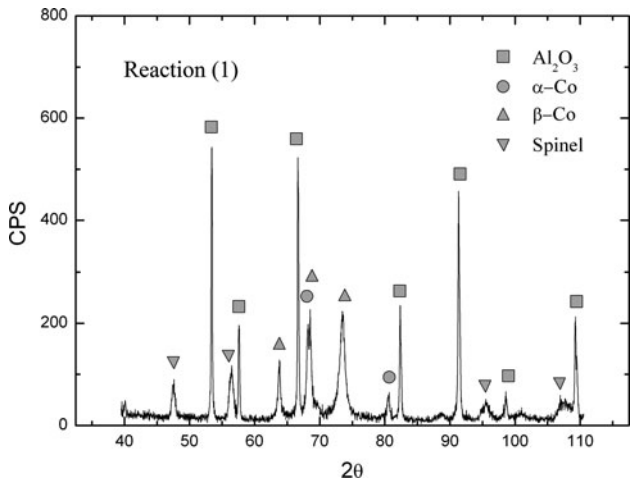

Fig. 3 XRD pattern for Al_2O_3–Co cermets

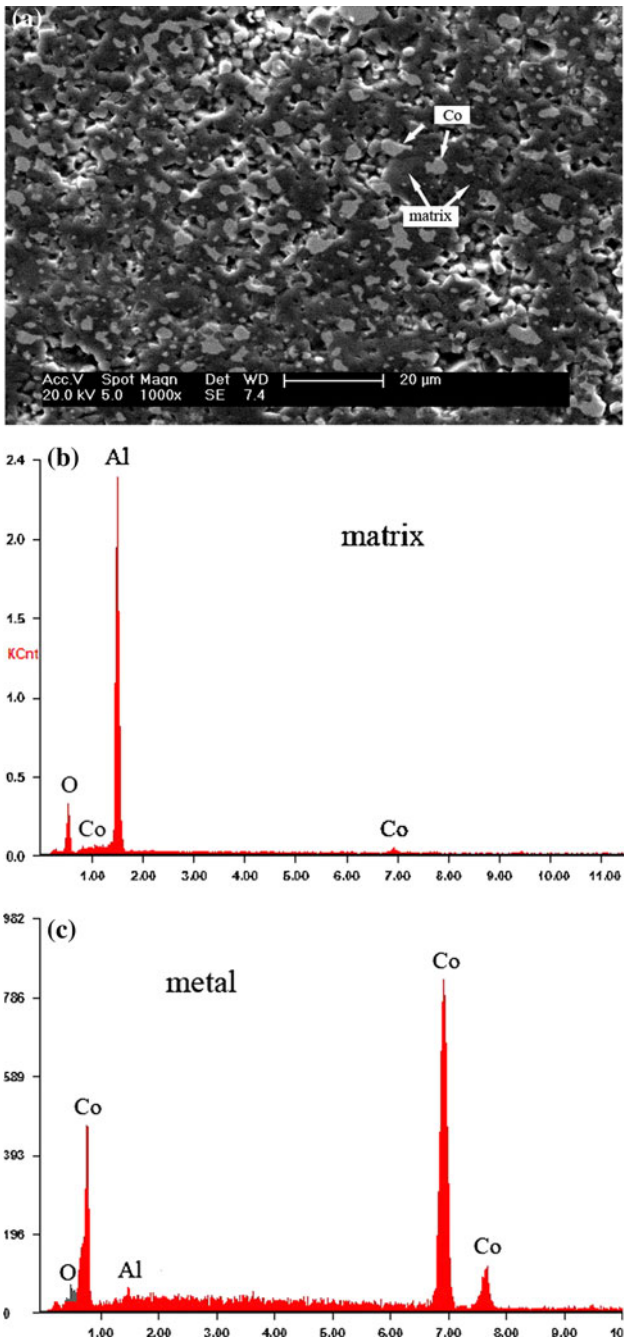

Fig. 4 SEM micrograph and EDS data for Al_2O_3–Co cermets

diluents absorbing a part of reaction heat and of the rapid heat loss after reaction. Meanwhile, most pores of the cermets after reaction are filled up by hot and ductile products when the uniaxial loading is applied, but a small amount of residual micro-pores still exist in the matrix because the separate micro-pores formed by the residual gas in the green compacts and by the volume shrinkage during cooling process are not entirely eliminated under this condition.

Al_2O_3–(Co–50Ni) cermets

In addition to synthesis of Al_2O_3–Co cermets (reaction (1)), we use Al–NiO system (reaction (2)) and Ni powders (reaction (3)) combined with Al–CoO system to prepare Al_2O_3–(Co–50Ni) cermets. The XRD patterns for both reactions as shown in Figs. 5 and 6, respectively, indicate that Co–50Ni alloys are well synthesized and the peaks of unreacted Al, Co–Al, or Ni–Al alloys are not found. Meanwhile, the peaks of unexpected (Co, Ni)Al_2O_4 spinel phases are found in both XRD results. In synthesis process, the spinel phase formed by CoO and NiO with Al_2O_3 acts as an intermediate and then it reacts with residual liquid Al to form Al_2O_3 and Co–50Ni alloy at high temperature during the reaction. However, $NiAl_2O_4$ is difficult to be formed in reaction (3) due to Ni powders which cannot directly react with Al_2O_3 that explains the reduced intensity of spinel peaks.

Figures 7 and 8 show the microstructures of Al_2O_3–(Co–50Ni) cermets prepared by reaction (2) and reaction (3), respectively. The morphology of Co–50Ni particle is apparently different with that of Co particle in Al_2O_3–Co cermets. The network-like Co–50Ni alloy particles as shown in Fig. 7 distribute along the boundary of Al_2O_3 particles. Moreover, a part of Al_2O_3 particles are wrapped by the interpenetrating Co–50Ni alloys as shown in Fig. 8 when we increase the content of alloys, that is, the residual micro-pores and the boundary gaps of Al_2O_3 particles can be filled up and the relative density of cermets can be improved. Therefore, we consider that the synthesized liquid Co–50Ni alloys can spread out on the surface of solid Al_2O_3 particles, and then due to the effect of pressure, the alloys are squeezed by surrounding Al_2O_3 particles and

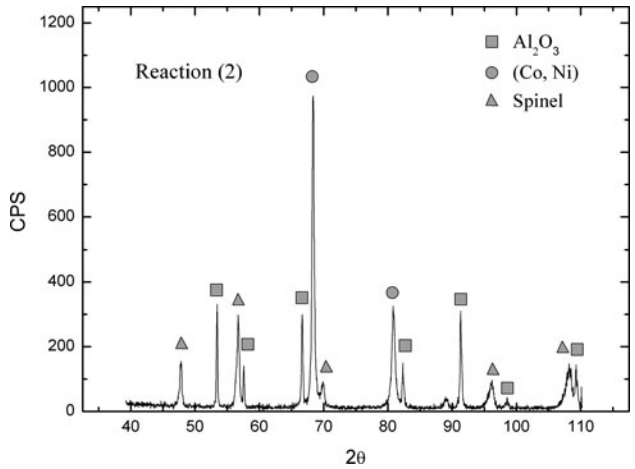

Fig. 5 XRD pattern for Al_2O_3–(Co–50Ni) cermets fabricated by reaction (2)

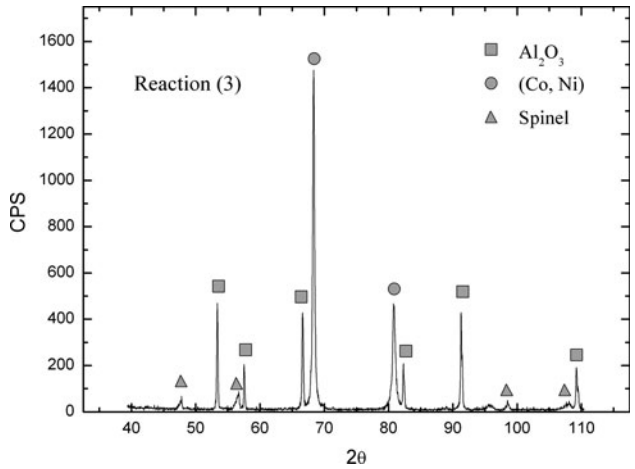

Fig. 6 XRD pattern for Al_2O_3–(Co–50Ni) cermets fabricated by reaction (3)

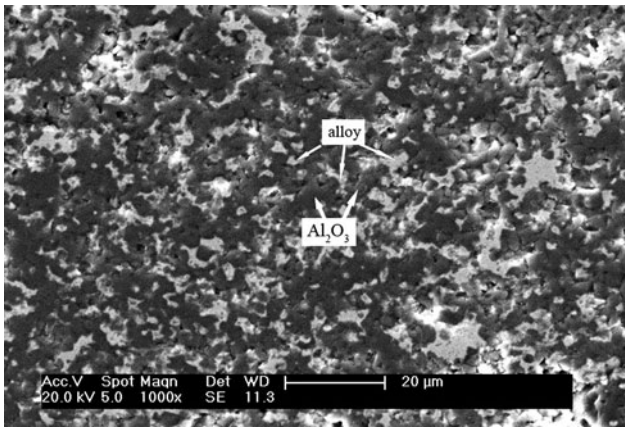

Fig. 7 SEM micrograph of Al_2O_3–(Co–50Ni) cermets fabricated by reaction (2)

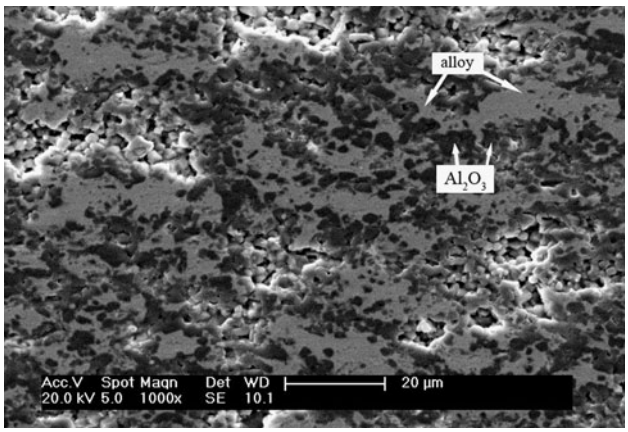

Fig. 8 SEM micrograph of Al_2O_3–(Co–50Ni) cermets fabricated by reaction (3)

finally can infiltrate into the boundary gaps to form network-like morphology during the cooling stage.

Magnetic properties

The magnetic hysteresis (M–H) loops of the cermets as shown in Figs. 9, 10, and 11, respectively, indicate that Al_2O_3–Co and Al_2O_3–(Co–50Ni) cermets are all ferromagnetic. Since Al_2O_3 is non-magnetic, the magnetic properties of cermets strongly depend on the magnetic Co and Co–50Ni phases. The parameters related to magnetic properties are summarized in Table 2. The lower saturation magnetization of Al_2O_3–Co cermets, which is about 42 emu/g and achieved for applied magnetic field that are above a value of 10 kOe or below a value of −10 kOe, is due to the β-Co preserved in the matrix which only presents magnetic property over 1121 °C. With incorporation of Ni, the saturation magnetizations of two kinds of Al_2O_3–(Co–50Ni) cermets are achieved for applied much lower magnetic fields. We consider that Al_2O_3–Co cermet is a kind of semi-hard magnetic composites, but Al_2O_3–(Co–50Ni) cermets represent soft magnetic property. Meanwhile, the saturation magnetization of Al_2O_3–(Co–50Ni) prepared by reaction (2) decreases to about 30 emu/g because the saturation magnetization of Co–50Ni alloy is lower than that of Co metal and more spinel phases are synthesized in the matrix. However, when we increase the content of magnetic Co–50Ni alloys in reaction (3), the saturation magnetization of Al_2O_3–(Co–50Ni) increases to about 48 emu/g.

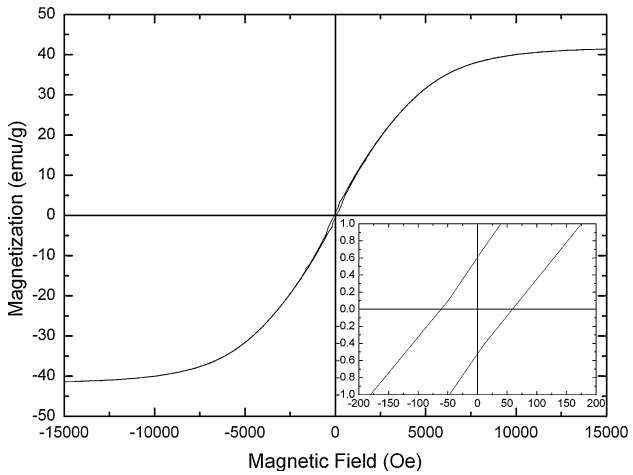

Fig. 9 The magnetic hysteresis (M–H) loops of Al_2O_3–Co cermets

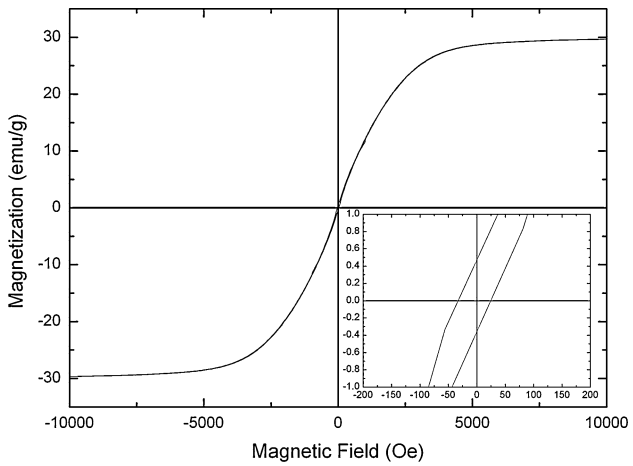

Fig. 10 The magnetic hysteresis (M–H) loops of Al_2O_3–(Co–50Ni) fabricated by reaction (2)

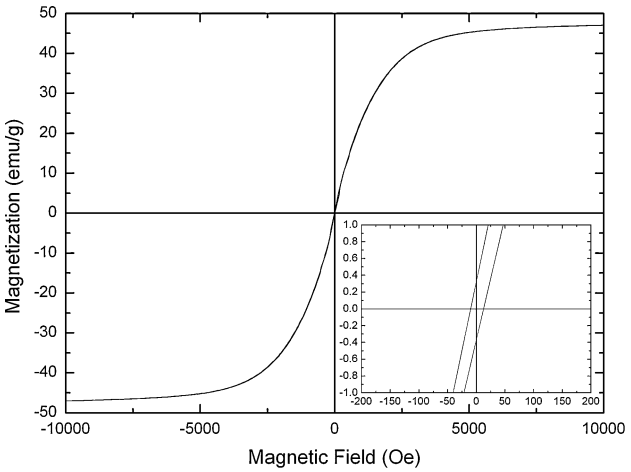

Fig. 11 The magnetic hysteresis (M–H) loops of Al_2O_3–(Co–50Ni) fabricated by reaction (3)

The coercive force is known to depend on the magnetic properties of the magnetic phases and on the grain size, residual stress, and dislocation density of the cermets [7]. The micro-scale Co–50Ni particles which represent soft magnetic property lead to the decrease of coercive force in Al_2O_3–(Co–50Ni) cermets. Moreover, the coercive force of the cermets prepared by reaction (3) further decreases to 11.17 Oe since the Co–50Ni particles become larger due to agglomeration and coalition when its content increases. We expect that nano-scale magnetic particles leading to a high coercive force can be prepared by this method in future study, for when the particle size of a magnetic material decreases, its magnetic structure varies from a multidomain state to a single-domain state, to reduce the total energy of the system [7]. In summary, the ferromagnetic Co–50Ni alloys are responsible of high magnetic susceptibility and low coercive force of Al_2O_3–(Co–50Ni) cermets.

Summary and conclusions

The ferromagnetic Al_2O_3–Co and Al_2O_3–(Co–50Ni) cermets were successfully prepared by combustion synthesis

Table 2 The parameters related to the magnetic properties

Cermets	Reactants	Saturation magnetization (emu/g)	Coercive force (Oe)
Al_2O_3–Co	Al–Co_2O_3–Al_2O_3	41.84	60.86
Al_2O_3–(Co–50Ni)	Al–Co_2O_3–NiO–Al_2O_3	29.96	28.48
Al_2O_3–(Co–50Ni)	Al–Co_2O_3–Ni–Al_2O_3	47.59	11.17

in thermal explosion mode. The production of dense cermets (relative density >95%) can be accomplished via uniaxial loading (about 1.28 MPa).

In Al_2O_3–Co cermets, in-situ synthesized Co particles disperse homogeneously in the matrix where β-Co and α-Co co-exist at room temperature. However, the shape of Co–50Ni alloy particle synthesized by Al–CoO system either with Al–NiO system or with direct adding of Ni powder becomes irregular and the alloys can infiltrate into the boundary of Al_2O_3 particles. Meanwhile, all of the cermets have a small quantity of residual spinel phases.

The analysis of magnetic properties shows that the saturation magnetization of Al_2O_3-based cermets strongly depends on the magnetic characteristic and ratios of Co and Co–50Ni. The ferromagnetic Co–50Ni alloys are responsible of high magnetic susceptibility and low coercive force of Al_2O_3–(Co–50Ni) cermets.

Acknowledgements An acknowledgement is due to associate professors Fan Li and Haibo Huang for the SEM facility and associate professor Xun Xiao for the XRD facility in Analysis and Testing Center of SEU. The authors also would like to thank to Mr. Xun Dong and Mr. Yancheng Zhang for the valuable discussions in the experiments.

References

1. Oh S-T, Sekino T, Niihara K (1998) J Eur Ceram Soc 18:31
2. Sekino T, Niihara K (1997) J Mater Sci 32:3943. doi: 10.1023/A:1018668900343
3. Nawa M, Sekino T, Niihara K (1994) J Mater Sci 29:3185. doi: 10.1007/BF00356661s
4. Qin XY, Cao R, Zhang J (2007) Compos Sci Tech 67:1530
5. Tai W-P, Kim Y-S, Kim J-G (2003) Mater Chem Phys 82:396
6. Aharon O, Bar-Ziv S, Gorni D, Cohen-Hyams T, Kaplan WD (2004) Scripta Mater 50:1209
7. Oh S-T, Sando M, Niihara K (1998) Scripta Mater 39:1413
8. Li J, Ni X, Wang G (2007) J Alloy Comp 440:349
9. Moore JJ, Feng HJ (1995) Prog Mater Sci 39:243
10. Khoptiar Y, Gotman I (2003) J Eur Ceram Soc 23:47
11. Hao J, Wang L (1994) Acta Metall Sin 30:45
12. Shi X, Pan Y, Guo J (2007) Ceram Int 33:1509